Investigation of compression ratio and fuel effect on combustion and PM emissions in a DISI engine

Lattimore, T. , Herreros, J. M. , Xu, H. and Shuai, S.

Original citation & hyperlink:
Lattimore, T. , Herreros, J. M. , Xu, H. and Shuai, S. (2016) Investigation of compression ratio and fuel effect on combustion and PM emissions in a DISI engine. Fuel, volume 169 : 68-78
http://dx.doi.org/10.1016/j.fuel.2015.10.044

DOI 10.1016/j.fuel.2015.10.044
ISSN 0016-2361
ESSN 1873-7153

Publisher: Elsevier

Investigation of Compression Ratio and Fuel Effect on Combustion and PM Emissions in a DISI Engine

Thomas Lattimore[1], Jose Martin Herreros[1], Hongming Xu[1,2*], Shijin Shuai[2]
1. University of Birmingham, Birmingham, B15 2TT, UK
2. State Key Laboratory of Automotive Safety and Energy, Tsinghua University, Beijing

Abstract

Oxygenated fuel components such as the alcohols of 1-butanol and ethanol are well-known for their potential to improve engine combustion and PM emissions, and these particular fuels are receiving ever greater attention due to their renewable nature giving them great CO_2 emission reduction potential. This paper investigates the effect of compression ratio and fuel properties on combustion, gaseous emissions and PM emissions of an experimental single-cylinder direct injection spark ignition (DISI) engine. The tests were carried out at an engine load of 8.5 bar, at various compression ratios between 10.7 and 11.5, with Bu20 (20%vol 1-butanol in gasoline) and E20 (20%vol ethanol in gasoline) fuel blends along with a reference fuel of gasoline. The results show that 1-butanol and ethanol addition to gasoline is effective to advance the MFB50 point and shorten the combustion duration. 1-butanol addition to gasoline is effective to reduce PM number emissions, while NO_x reduction is the main benefit of ethanol addition. It is concluded that synergies between compression ratio and alcohol addition to gasoline enable to simultaneously control gaseous and particulate matter emissions while improving fuel economy with respect to standard gasoline combustion.

Keywords: Compression Ratio; Butanol; DISI; Emissions; Particulates

* Corresponding author. Tel.: +44 121 4144153; fax: +44 121 4143958.

E-mail address: h.m.xu@bham.ac.uk (Hongming Xu).

1.0 Introduction

Reducing net CO_2 emissions from the transportation sector is at the forefront of public perception due to environmental protection concerns. One way to reduce engine CO_2 output is to increase engine's compression ratio; this improves its thermal efficiency causing the fuel consumption and thus CO_2 emissions to reduce. Another way to reduce net CO_2 output is to convert biomass to produce renewable oxygenated fuels to be used in the transportation and power generation sectors [1]. Furthermore the upcoming Euro 6 emissions regulations which limit for the first time the particulate number have increased interest in the effect of oxygenated fuels on engine particulates; they have the potential to significantly reduce particulate emissions having health benefits, particularly for people living in urban areas [2, 3]. The most commonly used biofuel component in spark ignition engines is ethanol; however there is increasing interest in the use of 1-butanol due to its higher calorific content, miscibility with gasoline, its water tolerance and its lower vapour pressure.

Gumbleton et al. [4] investigated the effect of compression ratio on engine performance and emissions in six vehicles with medium sized PFI gasoline engines. They found that increased compression ratio improved specific fuel consumption; something which was also reported by Ref. [5], [6], [7] and [8-11]. This is most likely due to the improved thermal efficiency achieved with the higher compression ratio. However Ref. [9] reported that BSFC got worse under low-speed, high-load conditions at high compression ratios due to spark retardation caused by heavy knocking with low octane gasoline. Nevertheless improvements were observed when a high octane gasoline was used at increased compression ratios [9].

Najafi et al. [12] investigated the effect of ethanol blended gasoline fuels on the performance and emissions of a 4-cylinder 1.3 litre SI engine. They observed that ethanol-gasoline

blended fuels increased the power (torque) of the engine across the engine load range because of the more advanced spark timings that could be achieved with ethanol blended fuel in comparison to gasoline. Ref. [13-17] reported similar findings. Brake specific fuel consumption improved; something which was attributed to the faster combustion of the ethanol fuel which increased the thermal efficiency of the engine. HC were observed to decrease with ethanol blending and NO_x was observed to increase. This was due to the enhanced oxidation and faster flame speed provided by the increased oxygen content of the ethanol fuel blend compared to gasoline. Ref. [13-15, 18-19] also observed HC emissions decrease with ethanol addition, however Ref. [20] observed no significant effect of ethanol blending on HC emissions. Ref. [14-15, 18-19, 21] observed NO_x emission decreases with ethanol addition, while Ref. [20] observed no significant effect of ethanol addition on NO_x emissions. Perhaps this was due to the spark timing not being advanced when the ethanol-gasoline fuel blend was used.

Deng et al. [22] studied the effect of 1-butanol blending on the performance and emissions of a single-cylinder PFI spark-ignition engine, using a 35%vol 1-butanol-gasoline blend; they compared this to a baseline of gasoline. They found that the ignition timing could be advanced with 1-butanol addition for higher thermal efficiency, due to the better knock suppression ability of 1-butanol fuel as compared to gasoline. The improved knock suppression ability has been attributed to the greater heat of vaporization of 1-butanol as compared to gasoline, giving it a greater charge cooling effect. Ref. [23-29] reported similar findings. Engine power (torque) and fuel consumption were found to have improved, with Ref. [25-26] and [28] reporting similar findings, due to the more advanced spark timings that could be achieved. Ref. [24], [26], [28] and [30-31] reported different findings however, with power and fuel economy observed to have decreased with increasing 1-butanol blended into

78 the gasoline fuel; most likely because the ignition timing was not advanced to its optimum
79 point when the 1-butanol-gasoline fuel blend was used. Gu et al. [32] studied the emission
80 characteristics of a 3-cylinder 0.8 litre PFI SI engine fuelled with 1-butanol-gasoline blended
81 fuels; they found that 1-butanol addition to gasoline reduced the particle number
82 concentration, due to the increased oxygen content of the 1-butanol fuel in comparison to
83 gasoline. Ref. [23], [26] and [33-34] reported similar findings for butanol-gasoline blends.
84 Ref. [23] reported that accumulation mode emissions showed the greatest reduction, most
85 likely because these larger particles were more affected by the higher rate of oxidation
86 achieved with the 1-butanol blended fuel, due to oxygen being present in its molecule.
87 However Ref. [35] reported that 1-butanol addition increased the particle number
88 concentration, which they attributed to poorer mixture formation.

89
90 Maji et al. [13] investigated the effect of the compression ratio using ethanol-gasoline blends
91 of 15 and 85%vol and a baseline fuel of gasoline on the performance and emissions of a
92 single-cylinder PFI engine. They found that as the compression ratio was increased, the HC
93 emissions increased for both gasoline and gasoline-ethanol blends; something which they
94 attributed to the increased surface to volume ratio of the combustion chamber. Ref. [6-7] and
95 [36] observed similar results with gasoline fuel; Ref. [7] attributed this to the higher relative
96 influence of the crevice volume compared to the whole volume of the combustion chamber as
97 well as in lower exhaust gas temperatures, supplying worse conditions for post-reactions of
98 HC in the exhaust pipe as the compression ratio was increased. As discussed, HC emissions
99 were also observed to have decreased with ethanol-gasoline fuel blends as compared to
100 gasoline, due to the increased oxidization provided by the oxygen atom in the ethanol
101 molecule.

102

Overall despite the amount of research that has been conducted into 1-butanol-gasoline and ethanol-gasoline blended fuels, there appears to be lack of agreement in terms of the effect these fuel blends on the combustion and emissions of gasoline engines. In addition, little work has been conducted regarding the effect of these fuel blends on the combustion and emissions of DISI engines with the majority of the research being conducted on PFI engines. Furthermore, 1-butanol-gasoline blended fuels have not been studied in detail in DISI engines, particularly their PM emissions. Finally, 1-butanol-gasoline and ethanol-gasoline fuel blends have not been studied well with each other along with a reference of gasoline fuel at different compression ratios. Therefore this research has been conducted to provide deeper knowledge about the effect of 1-butanol-gasoline and ethanol-gasoline blended fuels on combustion with focus on particulate matter (PM) emissions of DISI engines.

2.0 Experimental Setup and Procedure

2.1 Engine and Instrumentation

The specifications of the single cylinder DISI research engine used for the study are listed in Table 1, and the schematic is shown in Fig. 1. The engine was coupled to a direct current (DC) dynamometer and maintained at a constant speed of 1500 rpm (±1 rpm) regardless of the engine torque output. The in-cylinder pressure was measured using a Kistler 6041A water-cooled pressure transducer with a charge amplifier. Coolant and oil temperatures were maintained at 85°C and 95°C (±3°C) respectively, using a proportional integral differential (PID) controller and heat exchangers. All temperatures were measured with K-type thermocouples. The compression ratio was modified by adjusting the number and size of the metal inserts placed beneath the cylinder head. These acted to adjust the height of the cylinder head in relation to the piston BDC allowing the compression ratio to be changed. A

100 litre intake plenum tank (approximately 200 times the engine's swept volume) was used to stabilize the intake air flow.

Table 1 Experimental Single Cylinder Engine Specification

Parameter	
Engine Type	4-Stroke, 4-Valve
Combustion System	Spray Guided GDI
Swept Volume	565.6 cc
Bore x Stroke	90 x 88.9 mm
Engine Speed	1500 rpm
Engine Load	8.5 bar IMEP
DI Pressure and Injection Timing	15MPa, 280ºbTDC*
Intake Valve Opening	16.0ºbTDC**
Exhaust Valve Closing	36.0ºaTDC**

*TDC refers to TDC of combustion stroke, **TDC refers to TDC of exhaust stroke.

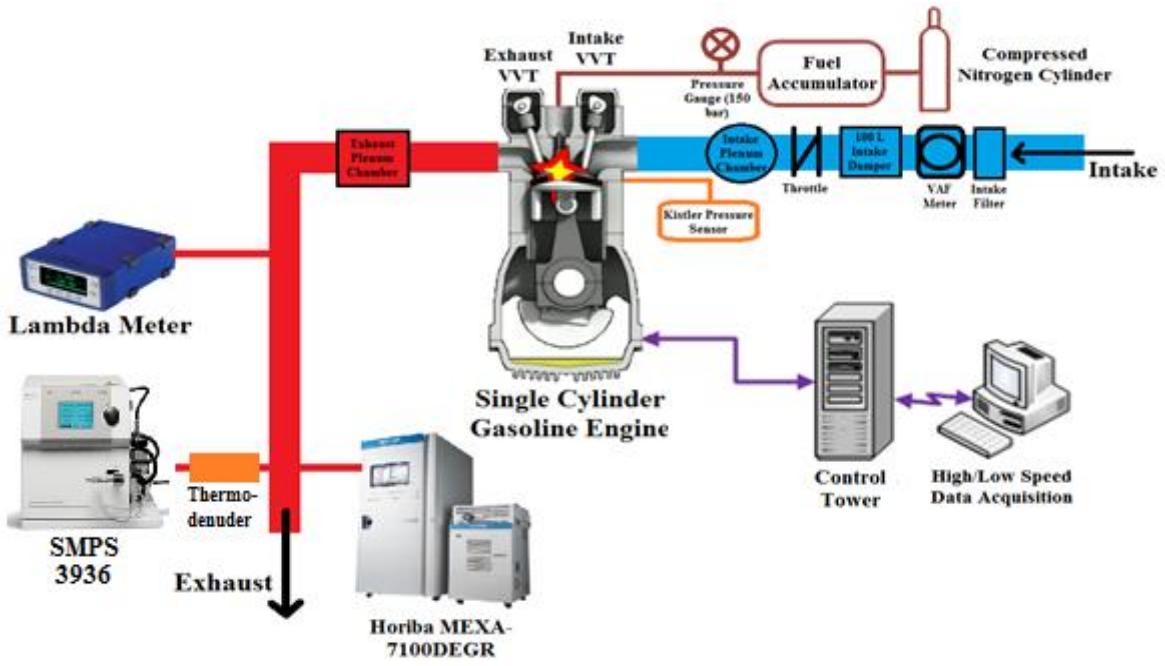

Fig. 1 Schematic of Engine and Instrumentation Setup **[Colour website, B&W print]**

Indicated fuel consumption was calculated from the measurement of the intake air flow rate which was made using the volumetric air flow meter (VAF). The load of 8.5 bar IMEP was chosen to study because it represents one of the worst conditions for engine knock in this

naturally aspirated (NA) engine, as well as being an engine load that is highly relevant for both NA and turbocharged DISI engines, increasing the usefulness of the data produced.

The engine cylinder head was a single-cylinder version of that used in the 2010 Jaguar LandRover AJ133 5.0 litre V8 engine. It was mounted on a modified single cylinder research engine and was not designed to be very resistant to knock. The engine has been used in this study for investigation of engine knocking phenomena. Therefore engine knock occurred at loads of 6.0 bar IMEP and above, which is somewhat lower than what can be expected with the state of the art aggressively downsized engines of modern cars on sale today. Furthermore, audible knock was observed to start occurring with 97 RON gasoline fuel at engine loads between 4.5 and 6.0 bar IMEP by previous researchers using this research engine [37-40]. Therefore the occurrence of knock at loads of 6.0 bar IMEP and above is consistent with these previous investigations.

The engine was controlled by an in-house program written in LabVIEW. All the engine operating data, pressure, and temperature data were acquired using another in-house LabVIEW program. For PM collection, the exhaust samples were taken 300 mm downstream of the exhaust valve of the engine, as indicated in the figure. They were then diluted by air (dilution ratio 4:1) at 150˚C to avoid condensation of the particulates, passed through a Topas TDD 590 thermodenuder at a temperature of 400˚C to remove most of the volatile nucleation mode particles and analysed in the Scanning Mobility Particle Sizer Spectrometer (SMPS3936) manufactured by TSI. The exhaust temperature at the sampling point was above 150˚C at all times, so that the particulates did not condense before they were sampled. For NO_x and HC emission measurement, the exhaust samples were taken opposite the PM sample point using the Horiba sampler device before being pumped via a heated line maintained at

190°C to the Horiba MEXA7100EGR emissions measurement system, where they were subsequently analysed.

A Labview program was developed in order to remove the unwanted noise from the pressure trace, to identify the knocking amplitude. The program read the on-line pressure data and applied a Butterworth second order type filter to isolate the frequency range of 4-12Hz, which ensured that the first and second harmonic knocking frequencies from the engine remained after the low and high frequency engine – generated signal noise had been removed. It then calculated the knocking amplitude from the amplitude of the filtered pressure trace. This provided on-line knocking amplitudes which allowed the KLMBT spark timing to be quantified at each engine condition before the engine data was recorded. The KLMBT was defined as the most advanced spark timing with 97% or more of the cycles having knock amplitudes below 2 bar. The maximum acceptable knock amplitude of 2 bar was chosen based on the work of Mittal et al. in Ref. [41]. If the maximum brake torque had been reached before the KLMBT timing, then this spark timing was defined as the KLMBT. Another in-house MatLab script was used to analyse the in-cylinder pressure trace along with other relevant parameters in order to calculate the MFB inside the combustion chamber; the same script was used in a previous publication by this research group [42].

The theoretical average in-cylinder temperatures were calculated using a detailed engine gas-dynamics and thermodynamics model used by the authors' research group in Ref. [1] and described in [37]. The model provides a good correlation between its simulated outputs and the experimental data. Fundamental assumptions made in the model are based on the information provided by Heywood [43]. Rather than using a relatively complex chemical kinetics model, the ideal gas law was used and combined with the prediction of trapped residuals and fuel vaporization behaviour to estimate the average in-cylinder gas temperature.

When simulating the combustion of gasoline, the fluid properties of indolene were used. When simulating the combustion of the fuel blends used, the known properties were inputted A primary combustion sub-model based on the recorded mass fraction burned (MFB) profile was used along with a SI Wiebe combustion sub-model which required the input of MFB50 and MFB10-90, in order to simulate the in-cylinder temperature conditions. In addition, a secondary sub-model was used based on the recorded pressure data to further enhance its precision. The model was validated using known combustion performance data to maintain the volumetric efficiencies to within 5% at all tested engine loads.

2.2 Test Fuels

The properties of the three studied fuels are listed in Table 2. Both gasoline and ethanol were supplied by Shell Global Solutions, UK. The 1-butanol was supplied by Fisher Scientific UK Ltd. The ULG95 was used in its supplied form, while the 1-butanol and ethanol fuels were mixed with the ULG95 fuel to form the Bu20 and E20 fuel blends with each containing 20%vol 1-butanol and 20%vol ethanol respectively. The ULG95 fuel was supplied with 5%vol ethanol pre-mixed in it, so the 20%vol 1-butanol blend and ULG95 fuel also had 5%vol ethanol in them too, while the 20%vol ethanol blend did not have any additional ethanol. It was chosen to study ethanol blended into gasoline fuel rather than in its pure form because ethanol is used on a wide scale only in its blended forms of up to 20%vol and in the near future this trend is likely to continue with ethanol-gasoline blends between 20-40%vol [20]. Therefore the blended form was tested which will not only allow the effect of ethanol addition to gasoline on DISI engine performance and emissions to be quantified, it will allow the precise effects of one of the most relevant ethanol-gasoline blends on DISI engine performance and emissions to be quantified. 1-butanol while not widely used in 1-butanol-gasoline blends has the potential to be used in the future with similar blend ratios as ethanol-gasoline blending; therefore 1-butanol has also been studied. It was studied in its Bu20 blend

213 with gasoline rather than its pure form due to the same reason ethanol was studied in its
214 blended form.

215 **Table 2** Test Fuel Properties

Parameter	Butanol	Ethanol	ULG95	Bu20	E20
Chemical Formula	$C_4H_{10}O$	C_2H_6O	C_2-C_{14}	C_2-C_{14}	C_2-C_{14}
H/C Ratio	2.5	3	1.922	2.038	2.084
O/C Ratio	0.25	0.5	0.021	0.067	0.093
Gravimetric oxygen content (%)	21.6	34.78	2.36	6.21	8.84
Density @ 20˚C (kg/m^3)	811	790.9*	743.9	757.3	753.3
Research Octane Number (RON)	98	106	95	-	102 [44]
Stoichiometric air–fuel ratio	11.2	8.95	14.15	13.71	13.78
LHV (MJ/kg)	32.71	26.9*	42.22	39.73	37.76
Initial boiling point, IBP (˚C)	118	78.4	34.6	34.6	34.6
Heat of Vaporization $\Delta_{vap}H$ (@ IBP) (kJ/kg)	585	858	373	-	-

216 * Measured at the University of Birmingham.

217

218 ## 2.3 Experimental Procedure

219 The engine was considered warmed-up once the coolant and lubricant temperatures were
220 stabilized at 85°C and 95°C respectively, and once the engine cylinder block had been
221 warmed to 95°C, as measured by a thermocouple embedded 5 mm within the block. Tests
222 were carried out at ambient air intake conditions (approximately 25°C). Indicated engine
223 loads were controlled by adjusting the throttle position and injection duration. Relative air-
224 fuel ratio λ was maintained at 1 during the experiments and a 5% COV of the IMEP was not
225 exceeded. Once the engine load condition had been achieved, 300 pressure cycles along with
226 engine emissions and particulate data were recorded. This procedure was then repeated for
227 the different engine fuel blends and reference fuel, and then again for the different
228 compression ratios. The test matrix for this investigation shown in Table 3 comprised an
229 overall number of 12 measurements. Readings for each measurement were taken
230 consecutively until 3 consistent readings were recorded. For the data presented in Fig. 3 and
231 6, the averaged data from the 3 readings was plotted along with the 95% confidence intervals,

in order to enable the significant effects of compression ratio and fuel on the data to be identified. The confidence intervals were calculated using equation (1).

$$CI = \bar{x} \pm Z_{\alpha/2} * \frac{\sigma}{\sqrt{n}} \qquad (1)$$

where CI = confidence interval, $\bar{x}$ = mean, $Z_{\alpha/2}$ = factor based on the desired confidence interval of 95%, which is 1.96, σ = standard deviation and n = sample size.

Table 3 Experiment Test Matrix

Compression Ratio / Fuel	10.7	10.9	11.2	11.5
Bu20	1	2	3	4
E20	5	6	7	8
ULG95	9	10	11	12

3.0 Results and Discussion

3.1 KLMBT Spark Timing

From the knock limited maximum brake torque (KLMBT) spark timings in Table 4, it can be seen that in the case of gasoline, an increase in the compression ratio had no significant effect on KLMBT. The same trend is also obtained for the butanol blend (similar octane rating than gasoline) and even for the ethanol blend, despite the high octane rating of ethanol. This is because at the engine load of 8.5 bar IMEP, the engine was very prone to knock, even in the case of alcohols, due to the high low temperature reactivity of alcohols [44] and the higher amount of fuel being injected into the combustion chamber (i.e. ethanol has lower calorific value than butanol and gasoline). Thus despite the compression ratio changing, no change in the KLMBT spark timing could be realized.

It can also be seen that more advanced KLMBT spark timings could be achieved with Bu20 and E20 as compared to ULG95, with the most advanced spark timings being achieved with Bu20. This is due to their higher octane number and the superior charge cooling effect of

alcohols compared to gasoline. Despite ethanol having a higher octane number than 1-butanol and cooling effect (in terms of mass), a more advanced KLMBT spark timings could be achieved with Bu20. It is believed that the 5%vol ethanol content in the Bu20 blend (20%vol 1-butanol with 5%vol ethanol) was sufficient to compensate for the lower charge cooling and octane number effect of 1-butanol as compared to ethanol. It is also thought that the higher chemical reactivity [44], faster laminar flame speeds and shorter fuel injection duration (less fuel quantity is required for the same engine output power due to the higher heating value than ethanol) for the butanol blend with respect to ethanol blend meant that the end-zone auto-ignition sites were consumed before they had an opportunity to auto-ignite, thus also contributing to the KLMBT spark advances.

Table 4 KLMBT Spark Timings (˚bTDC)

Compression Ratio / Fuel	10.7	10.9	11.2	11.5
Bu20	14˚	14˚	14˚	14˚
E20	12˚	12˚	12˚	12˚
ULG95	10˚	10˚	10˚	10˚

3.2 In-Cylinder Pressures and Temperatures, and Mass Fraction Burned (MFB)

The in-cylinder pressure traces for the two fuels blends of Bu20 and E20 along with that for the ULG95 reference fuel are shown in Fig. 2a, 2b, and 2c respectively. It is clear that as the compression ratio was increased, the maximum in-cylinder pressure increased, for the two fuel blends and the reference fuel tested. This is because the more compact combustion chamber achieved through the compression ratio increase, reduced the heat losses to the surroundings, resulting in the in-cylinder pressure increases. The in-cylinder pressures were highest for Bu20, followed by E20, then ULG95. This is due to the more advanced KLMBT spark timings which could be achieved with Bu20 and E20 as compared to those achieved

with ULG95, with the most advanced spark timings being achieved for Bu20; these are shown in Table 4. This made the combustion quicker and more efficient as the MFB50 point was advanced towards its optimum 8-10˚aTDC phase [45], as shown in Fig. 3a, resulting in the higher in-cylinder pressures observed.

Fig. 2d, 2e and 2f show the calculated average in-cylinder temperatures for the two fuel blends of Bu20 and E20 and for the reference fuel of ULG95, respectively. Overall the calculated average in-cylinder temperature increased as the compression ratio was increased. This is because of the aforementioned increase in in-cylinder pressure which resulted from the more compact combustion chamber achieved with the compression ratio increase. The calculated average in-cylinder temperatures were highest for ULG95, with Bu20 and E20 having lower but similar calculated average in-cylinder temperatures across the compression ratio range. It is proposed that this is due to the higher heat of vaporization of 1-butanol and ethanol as compared to ULG95, as shown in Table 2. This meant that more energy was required to vaporize these fuels, causing the average in-cylinder temperatures to reduce. The earlier start of combustion (advanced KLMBT and higher chemical reactivity) and especially the quicker combustion speed of butanol with respect to ethanol also contributed to the lower average in-cylinder temperatures.

The MFB profiles for the two tested fuel blends of Bu20 and E20, and the reference fuel of ULG95 are shown in Fig. 2g, 2h and 2i, respectively. For E20 there are no significant differences between the profiles at the different compression ratios while Bu20 and ULG95 show a slightly advanced combustion as the compression ratio was increased. It is proposed that the more highly compressed fuel-air mixture at the higher compression ratio burned more quickly than the less highly compressed mixtures at the lower compression ratios, causing the combustion to proceed more quickly. Despite this, it appears that the last stage of combustion

303 (less than 10% of the fuel mass remaining) was faster at lower compression ratios for all three
304 fuels. For a quantitative analysis of the combustion speed MFB10, MFB50 and MFB90 has
305 been calculated from the MFB profiles (please see next section).
306

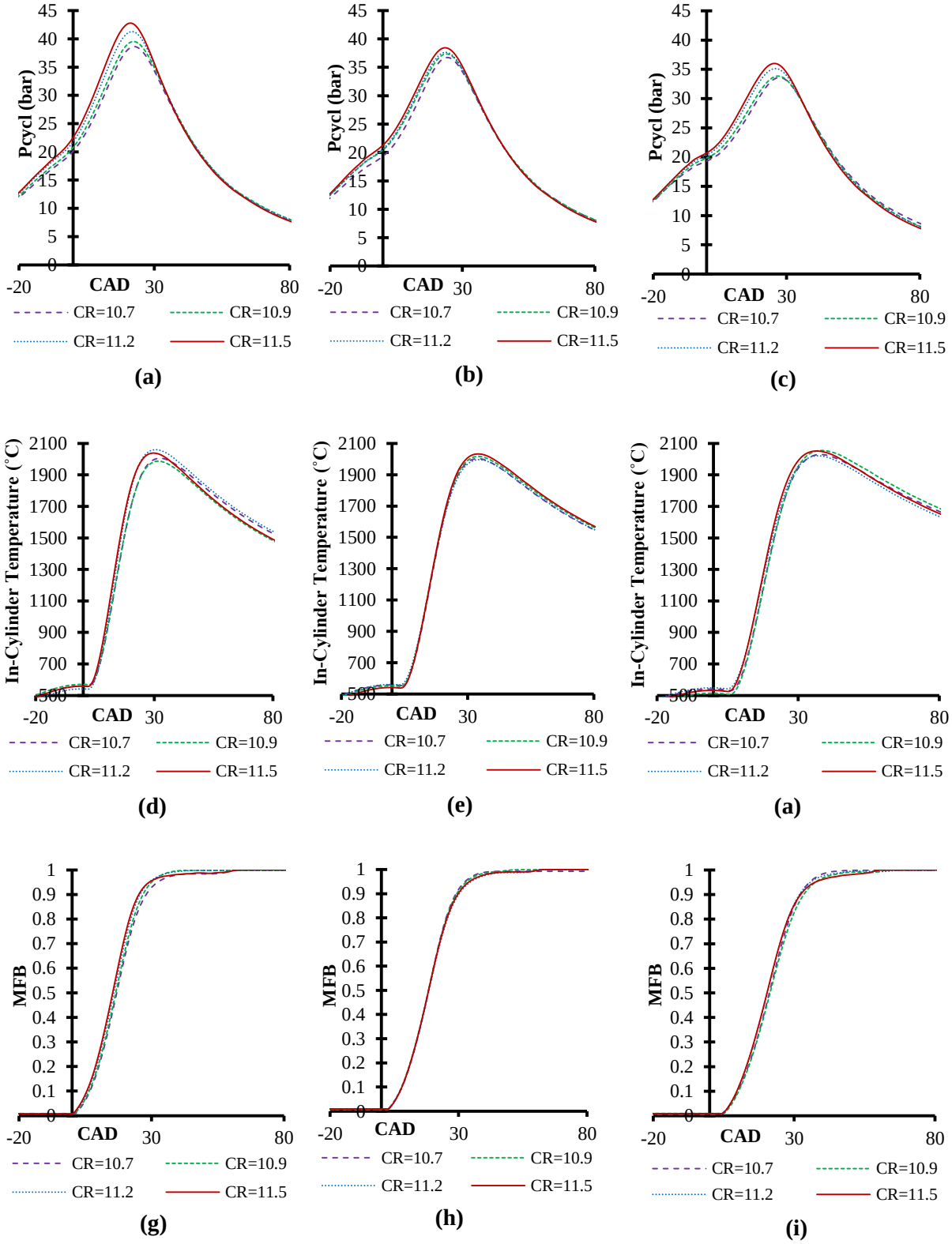

307 **Fig. 2** In-Cylinder Pressures versus CAD for **a)** Bu20, **b)** E20 and **c)** ULG95 at KLMBT spark timings;
308 calculated (estimated) average In-Cylinder Temperatures versus CAD at KLMBT spark timings for **d)** Bu20, **e)**
309 E20 and **f)** ULG95; MFB versus CAD at KLMBT spark timings for **g)** Bu20, **h)** E20 and **i)** ULG95 **[Colour**
310 **website, B&W print]**

3.3 MFB50, MFB10-90, Exhaust Gas Temperature and Indicated Efficiency

Fig. 3a shows the MFB50 data for the two tested fuel blends of Bu20 and E20, and the tested reference fuel of ULG95, across the compression ratio range. As discussed and explained previously, the KLMBT spark timings were most advanced for Bu20, with E20 second and ULG95 third, thus leading to the most advanced MFB50 of Bu20 across the compression ratio range, followed by E20 and ULG95. The MFB50 remained almost constant across the compression ratio range for E20; this is reflected in the MFB profile for E20 presented in Fig. 2h. However for the other two fuels of B20 and ULG95, there was a significant reduction in the MFB50 across the compression ratio range.

Fig. 3b shows the MFB10-90 data for the two tested fuel blends of Bu20 and E20, and the tested reference fuel of ULG95, across the compression ratio range. 1-butanol and ethanol addition to gasoline reduced the combustion duration of the fuel; it is proposed that 1-butanol and ethanol increased the linear flame speed, due to the oxygen in their molecule. The higher chemical reactivity of 1-butanol as compared to ethanol and the shorter injection duration of Bu20 with respect to E20 explains its shorter combustion duration in comparison. It has to be also noted that the combustion duration of Bu20 reduced significantly across the compression ratio range; this continues the trend in Fig. 3b which shows that the first half of the combustion process also proceeded more quickly across the range.

Fig. 3c shows the exhaust gas temperatures for the two tested fuel blends of Bu20 and E20, and the tested reference fuel of ULG95 across the compression ratio range. It is clear to see that there is general small decrease in exhaust gas temperatures across the compression ratio range. It is proposed that as the compression ratio increased and the MFB50 became advanced to its optimum 8-10˚aTDC CA50 point [45], the pressure and heat was more efficiently converted into work on the piston leading to the exhaust gas temperature decreases

across the compression ratio range [20]. Ref. [7] also observed exhaust gas temperature reductions as compression ratio was increased. The results also show that ULG95 had the highest exhaust gas temperature for all compression ratios, followed by E20, then Bu20. It is proposed that the more advanced MFB50 point of Bu20 as compared to ULG95 and E20 shown in Fig. 3a resulted in more efficient conversion of the pressure and heat into work on the piston, resulting in the reduced exhaust gas temperatures in comparison. Also as shown in Fig. 3a, the MFB50 point was more advanced for E20 than ULG95 for all compression ratios leading to lower exhaust gas temperatures in comparison, again due to more efficient conversion of the pressure and heat into work on the piston. The lower calculated average in-cylinder temperatures for the Bu20 and E20 fuel blends due to their higher heat of vaporization as compared to ULG95, will have also contributed to their lower exhaust gas temperatures, in comparison.

The indicated efficiency for the two tested fuel blends of Bu20 and E20, and the tested reference fuel of ULG95, across the compression ratio range, is shown in Fig. 3d. This was quantified by calculating the work output from the engine, then dividing it by the heat input from the fuel. They increased by 1.26%, 1.30% and 1.14% for Bu20, E20 and ULG95, respectively. This compares to a maximum theoretical thermal efficiency increase of 1.80% which can be obtained from equation (2) by assuming γ=1.4 and solving for the minimum and maximum respected compression ratios of 10.7 and 11.5.

$$n_{th=1-\frac{1}{r^{\gamma-1}}} \quad (2)$$

Therefore the thermal efficiency increase observed is realistic. As the compression ratio is increased, indicated (thermal) efficiency increases, thus producing the observed behaviour. Bu20 had the highest indicated efficiency, followed by E20 then ULG95, due to their respected KLMBT spark timings (Table 4) and their respected combustion durations (Fig.

3b). The more advanced the spark timing and the faster the combustion, the more efficiently the fuel was converted into engine power, thus resulting in the indicated efficiency increases observed.

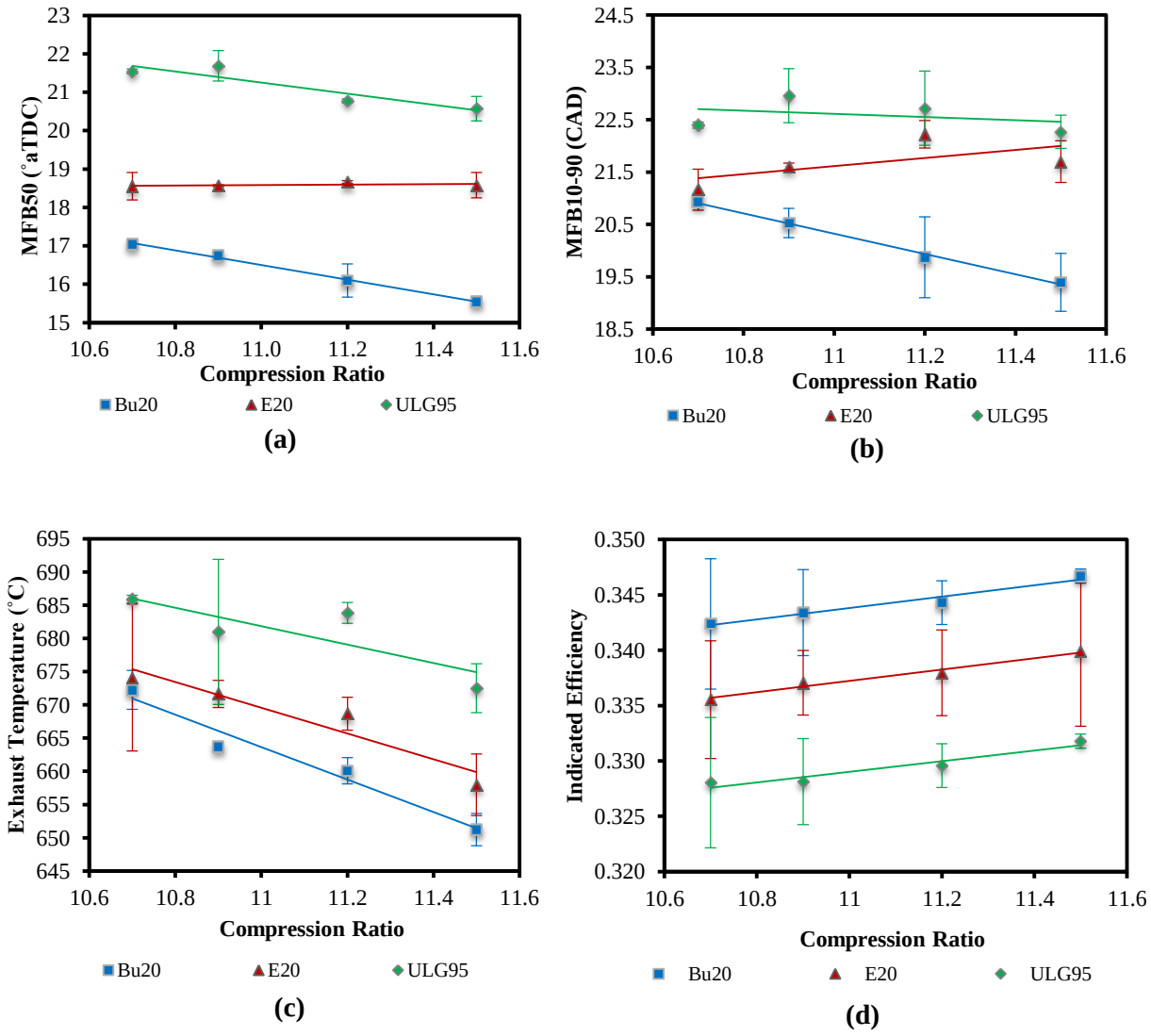

Fig. 3 Combustion parameters versus Compression Ratio at KLMBT spark timings **a)** MFB50, **b)** MFB10-90, **c)** exhaust Temperature, **d)** indicated Efficiency **[Colour website, B&W print]**

3.4 PM Emission Characteristics

3.4.1 Compression Ratio Effect on PM Number Emission

The particulate matter number emissions for the two tested fuel blends of Bu20 and E20, along with the tested reference fuel of ULG95 are shown in Fig. 4a, 4b and 4c, respectively. It is clear to see from Fig. 4a that compression ratio increase reduced the smaller nucleation mode particles on the left-hand side of the plot (3-30nm) for Bu20 blend. According to Ref. [24], the nucleation mode particles mainly result from droplets formed by hydrocarbon condensation and the accumulation mode particles are mainly composed of carbonaceous agglomerates formed in local rich-fuel zones [46, 47]. It is proposed the observed reduction was due to the increased calculated average in-cylinder temperatures across the compression ratio range which increased the oxidation of the particles in the combustion chamber. The KLMBT spark timing was unchanged across the compression ratio range, therefore mixture preparation was not considered to have had an effect on the observed behaviour.

E20 showed a similar trend to Bu20 but it was much weaker; the nucleation mode particles decreased as the compression ratio was increased. Again it is proposed that the higher calculated average in-cylinder temperatures shown in Fig. 2e increased the rate of oxidation of these particles in the combustion chamber, leading to the observed trend. For both Bu20 and E20 no significant changes in accumulation mode particle numbers were observed. It is believed that the increased oxidization of particles resulting from the increased calculated average in-cylinder temperatures across the compression ratio range was cancelled out by increased rate of particle formation caused by the increase in primary carbon particle formation by thermal pyrolysis and dehydrogenation reactions [23], also resulting from the increased calculated average in-cylinder temperatures.

The data for ULG95 shows a completely uni-modal distribution with no significant nucleation mode particles being recorded. As the compression ratio was increased, the formation of accumulation mode particles on the right hand side of the plot (30-500nm) increased. It is proposed that the accumulation mode particles increased across the compression ration range for ULG95 because the increased calculated average in-cylinder temperatures increased the particle formation rate, as with E20 and Bu20. This appears to have overcome the effect of increased particle oxidization resulting from the higher calculated average in-cylinder temperatures. Again the KLMBT spark timing was unchanged across the compression ratio range, thus mixture preparation is not thought to have had an effect on the observations.

For the two tested fuel blends Bu20 and E20, along with the tested reference fuel ULG95, it is proposed that significant nuclei adsorption of nucleation particles onto the accumulation particles occurred and this along with the thermodenuder, which removed many of the nucleation particles before they could be measured, lead to the mostly uni-modal behaviour observed.

3.4.2 Fuel Effect on PM Number Emission

Comparing the behaviours of the different fuels in Fig. 4a, 4b and 4c, 1-butanol significantly reduced the particle number when added to the gasoline fuel, whereas ethanol had little or no effect. It is proposed that the significantly earlier MFB50 point and shorter combustion duration of Bu20 as compared to the other two fuels provided more time for oxidation of the particulates after the combustion process, leading to the significant particle number reduction. This appears to have overcome the advanced KLMBT spark timing, which may have provided benefits in increased post-combustion oxidation time, but, on the other hand, would have reduced the fuel-air mixing time; and reduced calculated average in-cylinder temperatures. These would have resulted in more areas with a high local equivalence ratio and a reduced oxidation rate in the combustion chamber, respectively, which alone would have led to an increase in accumulation mode particles. However the increased post-combustion oxidization time was clearly the stronger effect. Also it is important to note that reduced calculated average in-cylinder temperatures will have also reduced the soot formation rate through reducing the primary carbon particles formed by thermal pyrolysis and dehydrogenation reactions; thus this may have contributed to the reductions observed. In addition, it is thought that because the gasoline already had 5%vol ethanol content, the increase in ethanol content to 20%vol made little difference to the particle number behaviour.

Overall there is no significant effect of fuel type on the particles average size with all distributions peaking at around 60nm. Ref. [23], [26] and [32-34] also reported that 1-butanol addition to gasoline fuel reduced the particle number concentration, and Ref. [18-19] and [48-53] also observed the same for ethanol addition to gasoline fuel.

There are further reasons as to why the accumulation mode particles decreased with butanol addition to gasoline fuel. Firstly, the reduced calculated average in-cylinder temperatures caused the primary carbon particles formed by thermal pyrolysis and dehydrogenation reactions to decrease [23]. Secondly, there is a positive correlation between the accumulation mode particles and the polycyclic aromatic hydrocarbon (PAHs); the addition of alcohol to gasoline reduces the aromatic content of the fuel, thus it also caused the accumulation mode particles to decrease [23]. Thirdly, the oxygen content in the fuel blend leads to a lower formation rate of soot and also to a higher oxidation rate of soot [23]. Despite these reasons contributing significantly to the reduction in accumulation mode particles observed for the Bu20 fuel blend, they did not decrease significantly for the E20 fuel blend in comparison to the reference ULG95 fuel. Lastly, Bu20 had a noticeably higher number of nucleation mode particles than the other two fuels tested. It is thought that this was due to the lower soot accumulation mode particles observed, which meant less adsorption of the nucleation mode particles onto the accumulation mode particle surfaces occurred, leading to higher numbers being observed in comparison to E20 and ULG95.

Overall, the effect of 1-butanol addition to gasoline on PM emissions is significant when the 95% confidence intervals are taken into consideration, while ethanol addition to gasoline has no significant effect at the blend ratio tested. Fig. 5 provides a summary of the effects of compression ratio and fuel on PM number emissions.

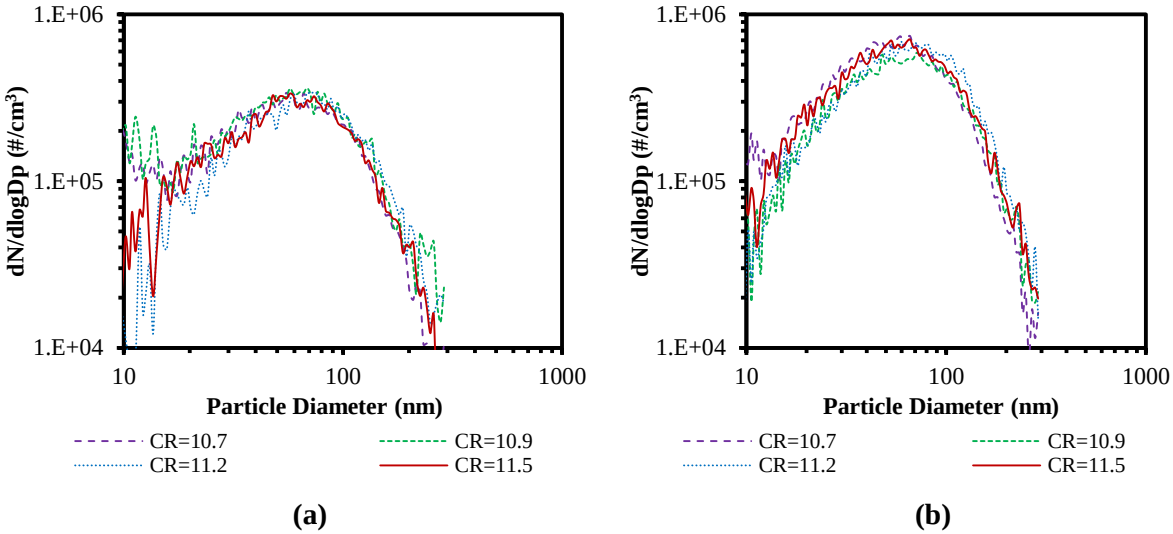

(a) **(b)**

456

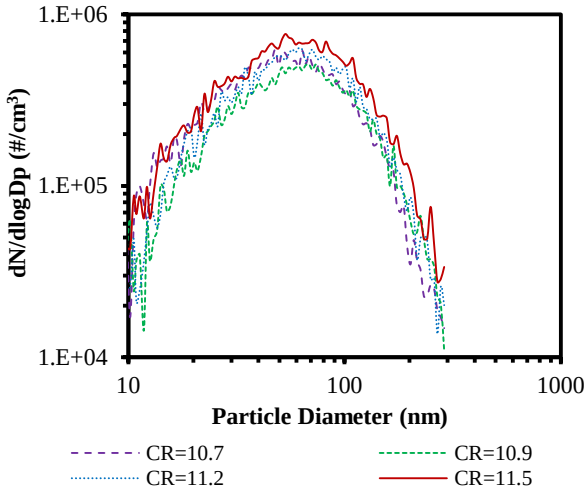

(c)

457

458 **Fig. 4** PM number emissions at KLMBT spark timings for **a)** Bu20, **b)** E20 and **c)** ULG95 **[Colour website,**
459 **B&W print]**

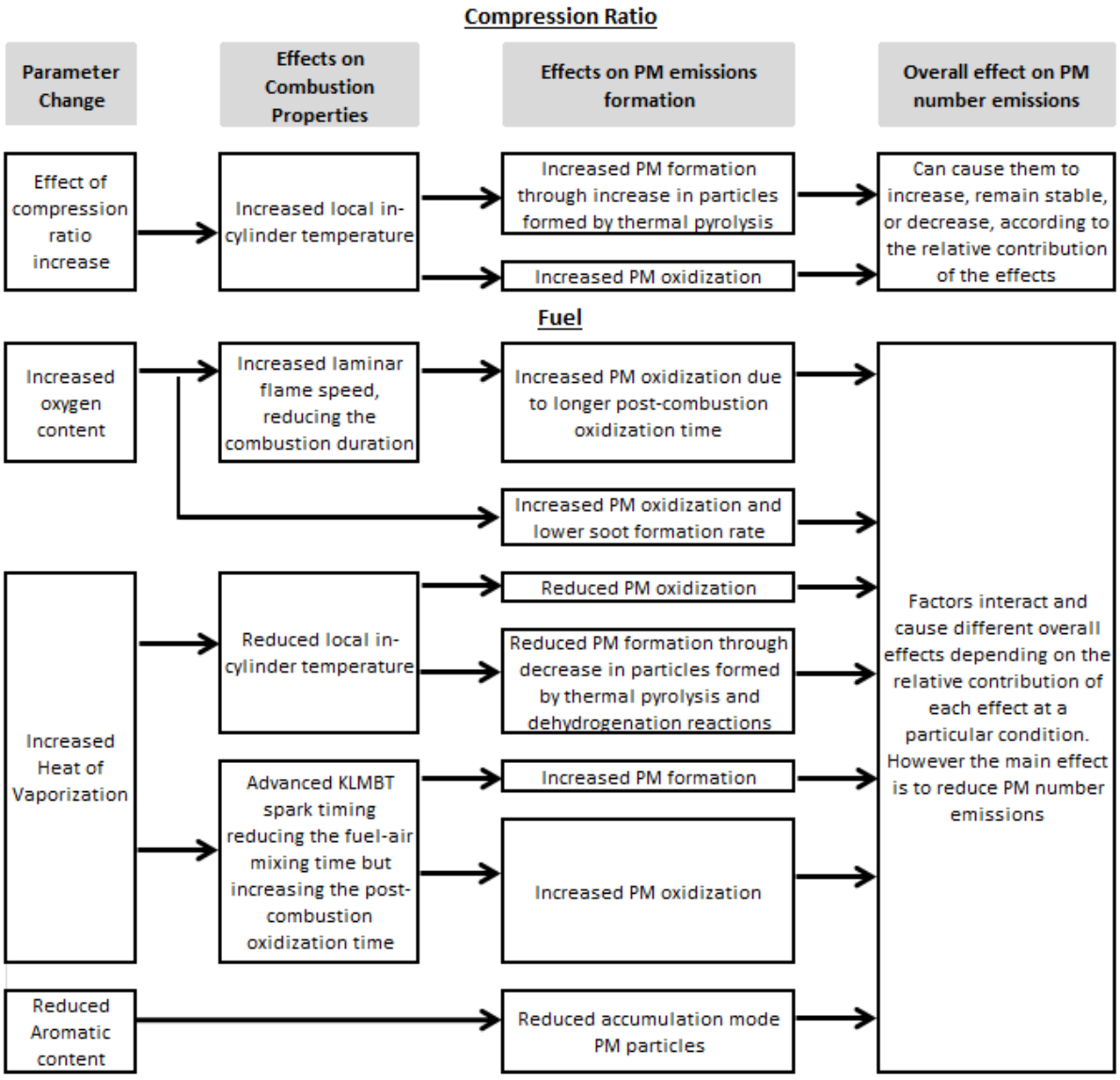

Fig. 5 Summary of the effects of compression ratio and fuel on PM number emissions **[B&W website, B&W print]**

3.5 NO_x and HC emissions

Fig. 6a presents the NO_x emission data for the two tested fuel blends and tested reference fuel. Overall there is a significant increase in NO_x emissions across the compression ratio range; they increased by 17.38% for Bu20, 21.69% for E20, and 23.51% for ULG95. These increases occurred because of the aforementioned increase in in-cylinder temperatures across the compression ratio range, which caused more NO_x to be formed. It is also clear that ULG95 had the highest NO_x emission, followed by Bu20 then E20. It is proposed that the lower calculated average combustion temperatures of Bu20 and E20 as shown in Fig. 2d and

2e, respectively, reduced the formation of NO_x emissions. Despite the calculated average in-cylinder temperatures being similar for Bu20 and E20 across the compression ratio change and ethanol having a higher O/C ratio than 1-butanol, Bu20 produced more NO_x emissions than E20. It is proposed that the earlier MFB50 of Bu20 as compared to E20, as shown in Fig. 3a, provided more time for NO_x to form in the hot flames, causing the higher NO_x emissions in comparison.

Fig. 6b presents the HC emissions data for the two tested fuel blends and the tested reference fuel. It is clear to see that the HC emissions increased significantly across the compression ratio range; they increased by 20.9% for Bu20, 20.8% for E20 and 26.2% for ULG95. It is suggested that the increased surface to volume ratio of the combustion chamber and the higher relative influence of the crevice volume as compared to the whole volume of the combustion chamber resulted in the observed HC emission increases [7, 13].

The emissions were lower for Bu20 and E20 as compared to ULG95 because their oxygen content was higher, which promoted the oxidation of HC in the combustion chamber. This appears to have overcome the reduced fuel-air mixing time caused by the more advanced KLMBT spark timing and the reduced combustion temperatures, which alone will have caused the HC emissions to increase. Ethanol has a higher oxygen to carbon ratio than 1-butanol, thus there was a higher HC oxidation rate of E20 as compared to Bu20, leading to lower HC emissions in comparison. Also the KLMBT spark timing was more advanced for the Bu20 fuel blend in comparison to E20, resulting in poorer mixture preparation and thus higher HC emissions. Finally the in-cylinder pressures were higher for Bu20 leading to more HCs being stored in the piston crevice area, contributing to the higher HC emissions observed for the Bu20 fuel blend.

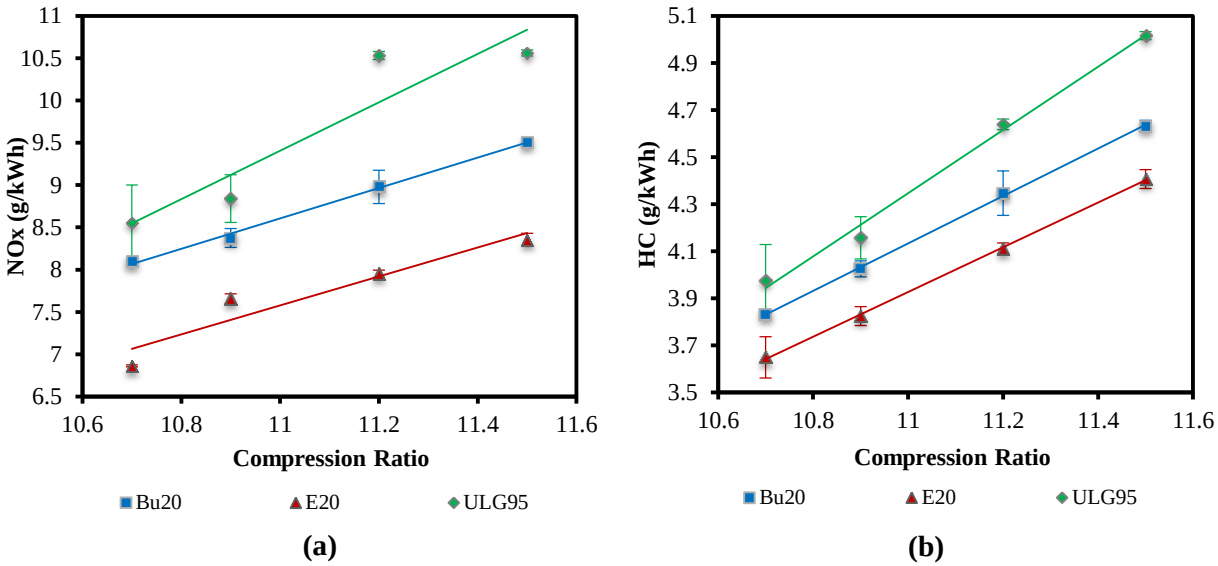

Fig. 6 Gaseous emissions versus Compression Ratio at KLMBT spark timings **a)** NO_x, **b)** HC **[Colour website, B&W print]**

3.6 Big Picture

Fig. 7 shows the overall effect of compression ratio and fuel on the gaseous emissions, indicated efficiency and total PN, while Fig. 8 summarises the compression ratio and fuel pathways affecting the combustion process, fuel economy and gaseous and particulate matter emissions. It is clear to see that for ULG95, the gaseous emissions of NO_x and HC increased with increased compression ratio, along with the indicated efficiency and total PN. However, when 1-butanol and ethanol are blended into the ULG95 fuel, the gaseous emissions of NO_x and HC are reduced, along with total PN, and the indicated efficiency is increased. Ethanol is most effective to reduce the gaseous emissions of NO_x and HC of the ULG95 fuel and 1-butanol is most effective to reduce the total PN emission.

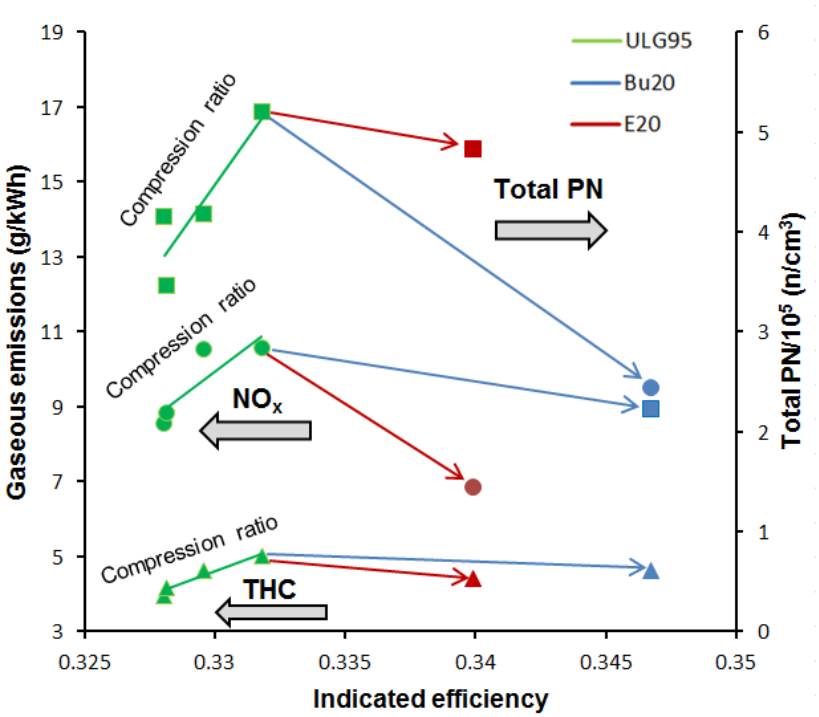

513

514 **Fig. 7** Overall effect of compression ratio and fuel on gaseous emissions, indicated efficiency and total PN
515 (integrated across 10-289nm range) at KLMBT spark timings **[Colour website, B&W print]**
516

517

4.0 Conclusions

The effect of compression ratio and fuel on combustion and PM emissions in a single cylinder DISI research engine was investigated in this paper and the following conclusions have been made.

1. 1-butanol and ethanol addition to gasoline advanced the MFB50 point as well as reducing the overall combustion duration across the compression ratio range; 1-butanol had the greatest effect on these parameters.
2. 1-butanol addition to gasoline significantly reduced the accumulation mode particulate number emission, due to the earlier combustion phasing and thus increased post-combustion oxidization time; ethanol addition to gasoline had little effect on the emission.
3. 1-butanol and ethanol addition to gasoline significantly reduced the NO_x and HC emission across the compression ratio range, with ethanol being the most effective.
4. Overall, if combustion and PM number emission parameters are the priority, then the Bu20 fuel blend has the most potential, while if NO_x and HC emission parameters are the priority, then the E20 fuel blend has the most potential. Synergies between compression ratio increase and alcohol addition to gasoline enable to simultaneously control gaseous and particulate matter emissions while increasing indicated efficiency with respect to standard gasoline combustion.

5.0 References

1. Wang, C., Xu, H., Daniel, R., Ghafourian, A., Herreros, J. M., Shuai, S. and Ma, X. (2013). Combustion characteristics and emissions of 2-methylfuran compared to 2,5-dimethylfuran, gasoline and ethanol in a DISI engine. Fuel. 103, 200-211, doi: http://dx.doi.org/10.1016/j.fuel.2012.05.043.
2. United States Environmental Protection Agency. (2014). Health. Available: http://www.epa.gov/pm/health.html. Last accessed 16th Jan 2015.
3. Anderson, J. O., Thundiyil, J. G., and Stolbach, A. (2012). Clearing the Air: A Review of the Effects of Particulate Matter Air Pollution on Human Health. Journal of Medical Toxicology. 8, 166-175, doi: 10.1007/s13181-011-0203-1.
4. Gumbleton, J., Niepoth, G. and Currie, J. (1976). Effect of Energy and Emission Constraints on Compression Ratio. SAE Technical Paper 760826, doi:10.4271/760826.
5. Harrington J. A. and Shishu R. C. (1973). A single-cylinder engine study of the effects of fuel type, fuel stoichiometry, and hydrogen-to-carbon ratio and CO, NO, and HC exhaust emissions. SAE 730476, doi: 10.4271/730476.
6. Muranaka, S., Takagi, Y. and Ishida, T. (1987). Factors Limiting the Improvement in Thermal Efficiency of S. I. Engine at Higher Compression Ratio. SAE Technical Paper 870548, doi:10.4271/870548.
7. Kramer, F., Schwarz, C. and Witt, A. (2000). Effect of Compression Ratio on the Combustion of a Pressure Charged Gasoline Direct Injection Engine. SAE Technical Paper 2000-01-0250, doi:10.4271/2000-01-0250.
8. Yin, T., Li, T., Chen, L. and Zheng, B. et al. (2014). Optimization of Compression Ratio of a Boosted PFI SI Engine with Cooled EGR. SAE Technical Paper 2014-01-2552, doi:10.4271/2014-01-2552.
9. Okamoto, K., Ichikawa, T., Saitoh, K. and Oyama, K. et al. (2003). Study of Antiknock Performance Under Various Octane Numbers and Compression Ratios in a DISI Engine. SAE Technical Paper 2003-01-1804, doi:10.4271/2003-01-1804.
10. Yamakawa, M., Youso, T., Fujikawa, T. and Nishimoto, T. et al. (2012). Combustion Technology Development for a High Compression Ratio SI Engine. SAE Int. J. Fuels Lubr. 5(1):98-105, doi:10.4271/2011-01-1871.
11. Smith, P., Heywood, J. and Cheng, W. (2014). Effects of Compression Ratio on Spark-Ignited Engine Efficiency. SAE Technical Paper 2014-01-2599, doi:10.4271/2014-01-2599.
12. Najafia, G., Ghobadiana, B., Tavakoli, T. (2009). Performance and exhaust emissions of a gasoline engine with ethanol blended gasoline fuels using artificial neural network. Applied Energy. 86, 630-639, doi:10.1016/j.apenergy.2008.09.017.
13. Maji, S., Babu, M. and Gupta, N. (2001). A Single Cylinder Engine Study of Power, Fuel Consumption and Exhaust Emissions with Ethanol. SAE Technical Paper 2001-28-0029, doi:10.4271/2001-28-0029.
14. Nakata, K., Utsumi, S., Ota, A. and Kawatake, K. et al. (2006). The Effect of Ethanol Fuel on a Spark Ignition Engine. SAE Technical Paper 2006-01-3380, doi:10.4271/2006-01-3380.
15. Taniguchi, S., Yoshida, K. and Tsukasaki, Y. (2007). Feasibility Study of Ethanol Applications to A Direct Injection Gasoline Engine. SAE Technical Paper 2007-01-2037, doi:10.4271/2007-01-2037.

16. Nakama, K., Kusaka, J. and Daisho, Y. (2009). Effect of Ethanol on Knock in Spark Ignition Gasoline Engines. SAE Int. J. Engines 1(1):1366-1380, doi:10.4271/2008-32-0020.
17. Overington, M. and Thring, R. (1981). Gasoline Engine Combustion—Turbulence and the Combustion Chamber. SAE Technical Paper 810017, doi:10.4271/810017.
18. Costagliola, M. A., De Simio, L., Iannaccone, S. and Prati, M. V. (2013). Combustion efficiency and engine out emissions of a S.I. engine fueled with alcohol/gasoline blends. Applied Energy. 111, 1162-1171, doi: http://dx.doi.org/10.1016/j.apenergy.2012.09.042.
19. Catapano, F., Di Iorio, S., Sementa, P. and Vaglieco, B. (2014). Characterization of Ethanol-Gasoline Blends Combustion processes and Particle Emissions in a GDI/PFI Small Engine. SAE Technical Paper 2014-01-1382, doi:10.4271/2014-01-1382.
20. Stein, R., Anderson, J. and Wallington, T. (2013). An Overview of the Effects of Ethanol-Gasoline Blends on SI Engine Performance, Fuel Efficiency, and Emissions. SAE Int. J. Engines 6(1):470-487, doi:10.4271/2013-01-1635.
21. Kar, K., Cheng, W. and Ishii, K. (2009). Effects of Ethanol Content on Gasohol PFI Engine Wide-Open-Throttle Operation. SAE Int. J. Fuels Lubr. 2(1):895-901, doi:10.4271/2009-01-1907.
22. Deng, B., Yang, J. and Zhang, D. (2013). The challenges and strategies of butanol application in conventional engines: The sensitivity study of ignition and valve timing. Applied Energy. 108, 248-260, doi: http://dx.doi.org/10.1016/j.apenergy.2013.03.018.
23. Zhang, Z., Wang, T., Jia, M., Wei, Q., Meng, X. and Shu, G. (2014). Combustion and particle number emissions of a direct injection spark ignition engine operating on ethanol/gasoline and n-butanol/gasoline blends with exhaust gas recirculation. Fuel. 130, 177-188, doi: http://dx.doi.org/10.1016/j.fuel.2014.04.052
24. Popuri, S. and Bata, R. (1993). A Performance Study of Iso-Butanol-, Methanol-, and Ethanol-Gasoline Blends Using a Single Cylinder Engine. SAE Technical Paper 932953, doi:10.4271/932953.
25. Yang, J., Yang, X., Liu, J. and Han, Z. et al. (2009). Dyno Test Investigations of Gasoline Engine Fueled with Butanol-Gasoline Blends. SAE Technical Paper 2009-01-1891, doi:10.4271/2009-01-1891.
26. Niass, T., Amer, A., Xu, W. and Vogel, S. et al. (2012). Butanol Blending - a Promising Approach to Enhance the Thermodynamic Potential of Gasoline - Part 1. SAE Int. J. Fuels Lubr. 5(1):265-273, doi:10.4271/2011-01-1990.
27. Merola, S., Tornatore, C., Valentino, G. and Marchitto, L. et al. (2011). Optical Investigation of the Effect on the Combustion Process of Butanol-Gasoline Blend in a PFI SI Boosted Engine. SAE Technical Paper 2011-24-0057, doi:10.4271/2011-24-0057.
28. Stansfield, P., Bisordi, A., OudeNijeweme, D. and Williams, J. et al. (2012). The Performance of a Modern Vehicle on a Variety of Alcohol-Gasoline Fuel Blends. SAE Int. J. Fuels Lubr. 5(2):813-822, doi:10.4271/2012-01-1272.
29. Tornatore, C., Merola, S., Valentino, G. and Marchitto, L. (2013). In-Cylinder Spectroscopic Measurements of Combustion Process in a SI Engine Fuelled with Butanol-Gasoline Blend. SAE Technical Paper 2013-01-1318, doi:10.4271/2013-01-1318.
30. Wigg, B., Coverdill, R., Lee, C. and Kyritsis, D. (2011). Emissions Characteristics of Neat Butanol Fuel Using a Port Fuel-Injected, Spark-Ignition Engine. SAE Technical Paper 2011-01-0902, doi:10.4271/2011-01-0902.
31. Yang, J., Wang, Y. and Feng, R. (2011). The Performance Analysis of an Engine Fueled with Butanol-Gasoline Blend. SAE Technical Paper 2011-01-1191, doi:10.4271/2011-01-1191.

32. Gu, X., Huang, Z., Cai, J., Gong, J., Wu, X. and Lee, C.-f. (2012). Emission characteristics of a spark-ignition engine fuelled with gasoline-n-butanol blends in combination with EGR. Fuel. 93, 611-617, doi:10.1016/j.fuel.2011.11.040.
33. Karavalakis, G., Short, D., Hajbabaei, M. and Vu, D. et al. (2013). Criteria Emissions, Particle Number Emissions, Size Distributions, and Black Carbon Measurements from PFI Gasoline Vehicles Fuelled with Different Ethanol and Butanol Blends. SAE Technical Paper 2013-01-1147, doi:10.4271/2013-01-1147.
34. He, X., Ireland, J., Zigler, B. and Ratcliff, M. et al. (2010). The Impacts of Mid-level Biofuel Content in Gasoline on SIDI Engine-out and Tailpipe Particulate Matter Emissions. SAE Technical Paper 2010-01-2125, doi:10.4271/2010-01-2125.
35. Thewes, M., Müther, M., Brassat, A. and Pischinger, S. et al. (2012). Analysis of the Effect of Bio-Fuels on the Combustion in a Downsized DI SI Engine. SAE Int. J. Fuels Lubr. 5(1):274-288, doi:10.4271/2011-01-1991.
36. de Souza, M., Vianna, J., and Fraga, A. (1998). Study of an Engine Operating with Exhaust Gas Recirculation at Different Compression Ratios. SAE Technical Paper 982895, doi:10.4271/982895.
37. Zhong S., Daniel R., Xu H. and Wyszynski M.L. (2010). Combustion and emissions of 2,5-dimethylfuran in a direct-injection spark-ignition engine. Energy & Fuels. 24, 2891–2899 doi:10.1021/ef901575a.
38. Daniel, R., Tian, G., Xu, H. and Shuai, S. (2012). Ignition timing sensitivities of oxygenated biofuels compared to gasoline in a direct-injection SI engine. Fuel. 99, 72-82, doi: http://dx.doi.org/10.1016/j.fuel.2012.01.053
39. Daniel, R., Tian, G., Xu, H., Wyszynski, M. L., Wu, X. and Huang, Z. (2011). Effect of spark timing and load on a DISI engine fuelled with 2,5-dimethylfuran. Fuel. 90, 449-458, doi:10.1016/j.fuel.2010.10.008
40. Daniel, R., Wang, C., Xu, H. and Tian, G. (2012). Effects of Combustion Phasing, Injection Timing, Relative Air-Fuel Ratio and Variable Valve Timing on SI Engine Performance and Emissions using 2,5-Dimethylfuran. SAE Int. J. Fuels Lubr. 5(2):855-866, doi:10.4271/2012-01-1285.
41. Mittal, V., Revier, B. and Heywood, J. (2007). Phenomena that Determine Knock Onset in Spark-Ignition Engines. SAE Technical Paper 2007-01-0007, doi:10.4271/2007-01-0007.
42. Wu, X., Daniel, R., Guohong, T., Xu. H., Huang, Z. and Richardson, D. (2011). Dual-injection: The flexible, bi-fuel concept for spark-ignition engines fuelled with various gasoline and biofuel blends. Applied Energy. 88, 2305–2314, doi:10.1016/j.apenergy.2011.01.025.
43. Heywood, J. B. (1988). Internal Combustion Engine Fundamentals. McGraw-Hill Higher Education.
44. He, B.-Q., Liu, M.-B. and Zhao, H. (2015). Comparison of combustion characteristics of n-butanol/ ethanol–gasoline blends in a HCCI engine. Energy Conversion and Management. 95, 101–109.
45. de O. Carvalho, L., de Melo, T. and de Azevedo Cruz Neto, R. (2012). Investigation on the Fuel and Engine Parameters that Affect the Half Mass Fraction Burned (CA50) Optimum Crank Angle. SAE Technical Paper 2012-36-0498, doi:10.4271/2012-36-0498.
46. Kittelson, D. B. (1998). Engines and nanoparticles: a review. Journal of Aerosol Science. 29, 575–588, doi:10.1016/S0021-8502(97)10037-4.
47. Anderson, J., Leone, T., Shelby, M. and Wallington, T. et al. (2012). Octane Numbers of Ethanol-Gasoline Blends: Measurements and Novel Estimation Method from Molar Composition. SAE Technical Paper 2012-01-1274, doi:10.4271/2012-01-1274.

48. Storey, J., Barone, T., Norman, K., and Lewis, S. (2010). Ethanol Blend Effects On Direct Injection Spark-Ignition Gasoline Vehicle Particulate Matter Emissions. SAE Int. J. Fuels Lubr. 3(2):650-659, doi:10.4271/2010-01-2129.
49. Di Iorio, S., Lazzaro, M., Sementa, P., Vaglieco, B. et al. (2011). Particle Size Distributions from a DI High Performance SI Engine Fuelled with Gasoline-Ethanol Blended Fuels. SAE Technical Paper 2011-24-0211, doi:10.4271/2011-24-0211.
50. Vuk, C. and Vander Griend, S. (2013). Fuel Property Effects on Particulates In Spark Ignition Engines. SAE Technical Paper 2013-01-1124, doi:10.4271/2013-01-1124.
51. Catapano, F., Di Iorio, S., Lazzaro, M. and Sementa, P. et al. (2013). Characterization of Ethanol Blends Combustion Processes and Soot Formation in a GDI Optical Engine," SAE Technical Paper 2013-01-1316, doi:10.4271/2013-01-1316.
52. Ojapah, M., Zhao, H. and Zhang, Y. (2014). Effects of Ethanol on Performance and Exhaust Emissions from a DI Spark Ignition Engine with Throttled and Unthrottled Operations. SAE Technical Paper 2014-01-1393, doi:10.4271/2014-01-1393.
53. Bielaczyc, P., Szczotka, A. and Woodburn, J. (2014). The Impact of Fuel Ethanol Content on Particulate Emissions from Light-Duty Vehicles Featuring Spark Ignition Engines. SAE Int. J. Fuels Lubr. 7(1):224-235, doi:10.4271/2014-01-1463.

Abbreviations

Bu20	20%vol 1-butanol in gasoline
CAD	Crank Angle Degrees
COV	Coefficient of Variation
DC	Direct Current
DISI	Direct-Injection Spark-Ignition
E20	20%vol ethanol in gasoline
IMEP	Indicated Mean Effective Pressure
KLMBT	Knock Limited Maximum Brake Torque
MFB	Mass Fraction Burned
NA	Naturally Aspirated
PFI	Port Fuel Injection
PID	Proportional Integral Differential
PM	Particulate Matter
ULG	Unleaded Gasoline
VAF	Volumetric Air Flow

Acknowledgement

This work was conducted in the Future Engines and Fuels Lab at the University of Birmingham and financially supported by the Engineering and Physical Sciences Research Council (EPSRC) through the Research Grant EP/F061692/1. The authors are grateful to the Jaguar Land Rover plc, Shell Global Solutions UK plc and Cambustion Ltd. for their great technical support throughout the research work. Also great thanks are extended to the technicians of the University of Birmingham, Mr. Carl Hingley and Mr. Peter Thornton for their assistance in the experiments.

Contact Information

Prof. Hongming Xu
Head of Vehicle and Engine Technology Centre
School of Mechanical Engineering
University of Birmingham
Birmingham
B15 2TT, UK

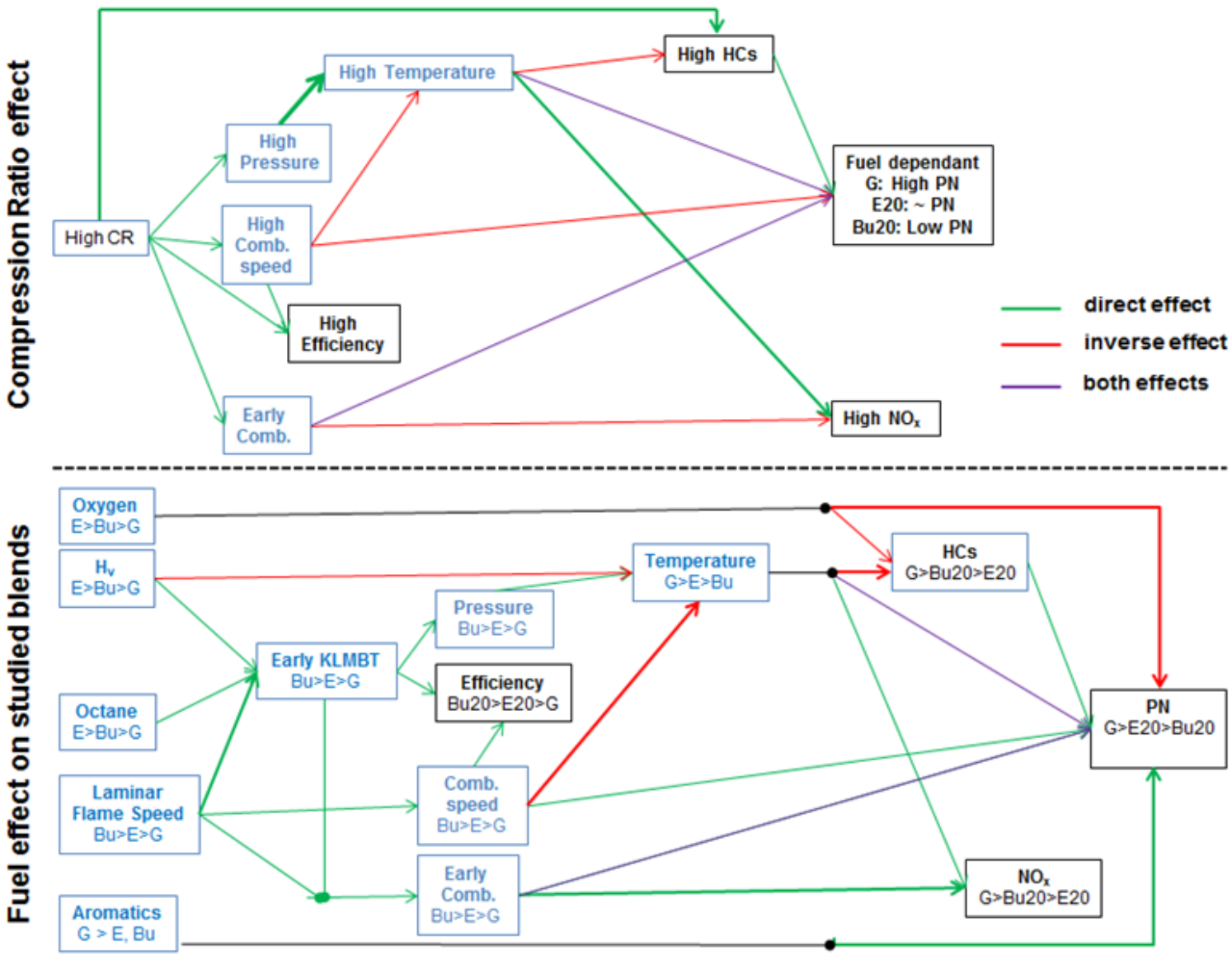

Fig. 8 Summary of compression ratio and fuel effects on combustion, fuel economy, gaseous and particulate matter emissions **[Colour website, B&W print]**